In a typical second-order experiment, a vial was charged with 1.00 mL of a benzene solution containing **1** or **7** and 0.05 molar equiv (with respect to Bu_3SnH) of AIBN. The vial was sealed and deoxygenated as described above and placed in a bath at 80 °C. After 15 min, the reaction was started by injecting the desired amount of Bu_3SnH. Reaction times of 1 h were used for both **1** and **7** at 80 °C.

Acknowledgment. We thank Dr. S. Brumby for computing assistance.

Note Added in Proof. In a private communication, Dr. J. Lusztyk has provided the following experimental Arrhenius parameters for the reaction of *tert*-butoxy radicals with Bu_3SnH: $E_a = 1.1 \pm 0.1$ kcal/mol, $\log (A/s^{-1}) = 9.5 \pm 0.1$. Although these values are in reasonable agreement with our earlier estimates of $E_a = 1.83 \pm 0.54$ kcal/mol and $\log (A/s^{-1}) = 9.70 \pm 0.40$,[6] they suggest that the value of $k_3 = 6.6 \times 10^8$ M^{-1} s^{-1} at 80 °C would be more correct than that (3.7×10^8 M^{-1} s^{-1}) used in the paper. In this case the values of k_{-1}, k_4, and k_{-6} at 80 °C should be increased correspondingly by a factor of 1.8.

Registry No. **1**, 1191-30-6; **2**, 78939-50-1; **3**, 53578-06-6; **4**, 110-62-3; **5**, 96-41-3; **6**, 71-41-0; **7**, 57978-00-4; **8**, 59282-49-4; **9**, 3384-35-8; **10**, 66-25-1; **11**, 108-93-0; **12**, 111-27-3; Bu_3SnH, 688-73-3; nonanal, 124-19-6; 5-hexenyl radical, 16183-00-9; cyclopentylcarbinyl radical, 119009-89-1.

D-Talose Anomerization: NMR Methods To Evaluate the Reaction Kinetics

Joseph R. Snyder,[†] Eric R. Johnston,[‡] and Anthony S. Serianni*,[†]

Contribution from the Department of Chemistry, University of Notre Dame, Notre Dame, Indiana 46556, and Department of Chemistry, Haverford College, Haverford, Pennsylvania 19041. *Received July 16, 1987*

Abstract: The kinetics of anomerization of the aldohexose, D-talose, have been studied by several NMR methods in order to evaluate their limitations, complementarity, and internal consistency and to further explore the effect of monosaccharide structure on reactivity. By use of D-[1-^{13}C]talose and ^{13}C NMR spectroscopy, six tautomeric forms were detected and quantitated in aqueous solution: α- and β-talofuranoses, α- and β-talopyranoses, hydrate (1,1-*gem*-diol), and aldehyde. The ^{13}C (75-MHz) and ^{1}H (620-MHz) NMR spectra of D-talose have been interpreted, yielding chemical shifts and coupling constants (J_{HH}, J_{CC}, J_{CH}) that have been evaluated in terms of ring configuration and conformation. By use of ^{13}C saturation-transfer NMR (ST-NMR), ring-opening rate constants (k_{open}) of the four cyclic forms were measured, and ring-closing rate constants (k_{close}) were calculated from k_{open} and equilibrium constants. NMR-derived rates of tautomer equilibration obtained after dissolving α-D-[1-^{13}C]talopyranose in aqueous solution were predicted accurately from a computer treatment of the unidirectional rate constants determined by ST-NMR under similar solution conditions. Two-dimensional ^{13}C exchange spectroscopy was applied to obtain overall rate constants of tautomer interconversion; rate constants obtained in this fashion compared favorably with those calculated from the ST-derived unidirectional rate constants using the steady-state approximation. Kinetic results show that anomeric configuration and ring size significantly affect ring-opening and ring-closing rates of monosaccharides.

Aldohexoses have the potential to exist in six monomeric forms (tautomers) in aqueous solution [α- and β-furanose, α- and β-pyranose, hydrate (1,1-*gem*-diol), and aldehyde].[1,2] The spontaneous interconversion between the cyclic forms, known as anomerization, appears to involve the aldehyde as an obligatory intermediate,[3,4] although its conformation has been the subject of debate.[5,6a,7] This characteristic reaction of reducing sugars plays an important role in organic chemistry and biochemistry. From the chemical standpoint, anomerization is an ideal reaction to assess the effects of structure, configuration, and conformation on ring-forming and ring-opening reactions in general, especially since many stereoisomers of the monosaccharides are available for study. In the biological sense, Benkovic and co-workers[6b] have shown that enzymes often act on specific tautomers of biologically important reducing sugars (e.g., D-fructose 6-phosphate). In some instances, therefore, the kinetics of tautomer interconversion can be a potential factor in regulating flux through certain pathways in cells.

Many studies[7-11] have examined the effect of carbohydrate and solvent structure on anomerization rates using various sugars, reaction conditions, and experimental protocols, producing a body of information that has established the general features of the reaction. Despite this considerable effort, however, little is known about the component ring-opening and ring-closing rate constants and their dependence on experimental conditions. This latter problem has been the focus of attention in this laboratory in recent years. With the aid of ^{13}C enrichment, we have shown that minor tautomers (e.g., hydrate and carbonyl forms) of monosaccharides can be detected and quantified in solution by ^{13}C NMR.[3b,4,12,13] Without enrichment, their detection is difficult. We have used ^{1}H and ^{13}C saturation-transfer NMR (ST-NMR)[3b,4,13,14] and

[†] University of Notre Dame.
[‡] Haverford College.

(1) Angyal, S. J. *Angew. Chem., Int. Ed. Engl.* **1969**, *8*, 157.
(2) Angyal, S. J. *Adv. Carbohydr. Chem. Biochem.* **1984**, *42*, 15.
(3) (a) Los, J. M.; Simpson, L. B.; Wiesner, K. *J. Am. Chem. Soc.* **1956**, *78*, 1564. (b) Serianni, A. S.; Pierce, J.; Huang, S.-G.; Barker, R. *J. Am. Chem. Soc.* **1982**, *104*, 4037.
(4) Pierce, J.; Serianni, A. S.; Barker, R. *J. Am. Chem. Soc.* **1985**, *107*, 2448.
(5) Isbell, H. S.; Frush, H. L.; Wade, C. W. R.; Hunter, C. E. *Carbohydr. Res.* **1969**, *9*, 163.
(6) (a) Wertz, P. W.; Garver, J. C.; Anderson, L. *J. Am. Chem. Soc.* **1981**, *103*, 3916. (b) Benkovic, S. J.; Schray, K. J. *Adv. Enzymol. Relat. Areas Mol. Biol.* **1976**, *44*, 139.
(7) Isbell, H. S.; Pigman, W. *Adv. Carbohydr. Chem. Biochem.* **1969**, *24*, 13.
(8) Pigman, W.; Isbell, H. S. *Adv. Carbohydr. Chem.* **1968**, *23*, 11.
(9) Livingstone, G.; Franks, F.; Aspinall, L. J. *J. Solution Chem.* **1977**, *6*, 203.
(10) Lemieux, R. U.; Anderson, L.; Conner, A. H. *Carbohydr. Res.* **1971**, *20*, 59.
(11) Capon, B.; Walker, R. B. *J. Chem. Soc., Perkins Trans. 2* **1974**, 1600.
(12) Barker, R.; Serianni, A. S. *Acc. Chem. Res.* **1986**, *19*, 307.
(13) Snyder, J. R.; Serianni, A. S. *J. Org. Chem.* **1986**, *51*, 2694.

0002-7863/89/1511-2681$01.50/0

NMR line-broadening methods[4] to determine unidirectional rate constants (k_{open}, k_{close}) in anomerizing systems. To broaden the future scope of our studies, we decided to apply several complementary NMR approaches to kinetic studies of anomerization of the aldohexose, D-talose, with the intent of evaluating their general applicability, limitations, and internal consistency. Two-dimensional ^{13}C exchange spectroscopy[15] has been examined as a means to obtain overall rate constants of talose tautomer interconversion (e.g., α-talopyranose $\rightarrow$ β-talofuranose). Time-lapse ^{13}C NMR spectra have been obtained after dissolution of crystalline α-D-[1-^{13}C]talopyranose to monitor the formation of the remaining talose tautomers; rates of equilibration obtained in this fashion have been compared to those predicted by computer[6a,16] using the unidirectional rate constants determined by ST-NMR.

The aldohexose, D-talose, was chosen for this study because (a) aqueous solutions of this monosaccharide at equilibrium contain comparable amounts of both furanose and pyranose forms, (b) the linear carbonyl form can be observed by ^{13}C NMR with D-[1-^{13}C]talose, and (c) α-talopyranose can be obtained in crystalline form. D-Talose is one of a few simple aldoses that possess these characteristics, one or more of which were required by the experimental methods used in this investigation.

Experimental Section

A. Preparation of α-D-[1-^{13}C]Talopyranose. D-[1-^{13}C]Talose was prepared from K^{13}CN (Cambridge Isotope Laboratories; 99 atom % ^{13}C) and D-lyxose (Sigma Chemical Co.) according to procedures described previously.[17,18] After reduction, the Pd–$BaSO_4$ catalyst was removed by suction filtration, and the filtrate was treated batchwise and separately with excess Dowex 50 × 8 (20–50 mesh) (H^+) and Dowex 1 × 8 (20–50 mesh) (HCO_3^-) ion-exchange resins. The deionized solution was concentrated at 30 °C in vacuo to ~15 mL and chromatographed on a 2.5 × 100 cm column of Dowex 50 × 8 (200–400 mesh) (Ca^{2+}) resin using distilled water as the solvent (1 mL/min).[19] Fractions (8 mL) were assayed for reducing sugar with phenol–sulfuric acid;[20] D-[1-^{13}C]galactose eluted first (fractions 35–69), followed by D-[1-^{13}C]talose (fractions 130–170). Fractions containing labeled talose were pooled and concentrated at 30 °C in vacuo to a syrup. α-D-[1-^{13}C]Talopyranose crystallized from the syrup with hot ethanol [mp 129–130 °C (lit.[21] mp 133 °C)].

B. Preparation of D-Talose, D-[3-^{2}H]Talose, and D-[1-^{13}C]Erythrose. D-Talose was prepared and purified as described above for D-[1-^{13}C]talose, substituting KCN for K^{13}CN in the synthesis.

D-[3-^{2}H]Talose was prepared by methods described in detail previously,[22] and only a general description is given here. D-Threose[23] was treated with KCN in ^2H_2O, and the resulting C2-epimeric cyanohydrins (lyxo, xylo) were reduced with Pd–$BaSO_4$ and $^2H_2$ gas.[18,22] The product D-[1-^{2}H]pentoses were separated by chromatography, and D-[1-^{2}H]xylose was epimerized with sodium molybdate[24] to generate a mixture of D-[1-^{2}H]xylose and D-[2-^{2}H]lyxose. After chromatography, D-[2-^{2}H]lyxose was converted to D-[3-^{2}H]talose as described above for the preparation of the 1-^{13}C-enriched derivative.

D-[1-^{13}C]Erythrose was prepared from D-glyceraldehyde and K^{13}CN and purified by chromatography as described previously.[25]

C. Instrumentation and Methods. ^1H (300-MHz) and ^{1}H-decoupled ^{13}C (75-MHz) NMR spectra were obtained on a Nicolet NT-300 FT-NMR spectrometer equipped with quadrature-phase detection, a 293B pulse programmer, and a 16-bit digitizer to improve dynamic range. Temperature (±1 °C) was measured with a Fluke 2160A digital thermometer by placing the thermocouple directly into an equilibrated (~15 min) NMR sample in the NMR probe.[3b,4]

Time-lapse ^{13}C spectra and 2D ^{13}C–^1H chemical shift correlated spectra[26] were obtained on the NT-300 NMR with previously tested[13] software supplied by GE NMR systems. ^{13}C saturation-transfer NMR (ST-NMR) spectra were obtained on the same spectrometer by using the hardware modifications and pulse program described previously,[13] and rate constants were calculated from a graphical treatment of the data.[3b,4] High-resolution rapid-scan cross-correlation ^1H NMR spectroscopy at 620 MHz was performed at the NMR Facility For Biomedical Studies, Department of Chemistry, Carnegie Mellon University, Pittsburgh, PA, which is partly supported by NIH Grant P41RR00292-19.

Phase-sensitive 2D ^{13}C exchange spectra were obtained on an IBM NR-80 NMR spectrometer operating at 20.02 MHz and located in the Department of Chemistry, Haverford College, Haverford, PA. The pulse sequence used to evaluate exchange rates was described previously by Johnston et al.,[27a] and only a general description is given here. A total of 256 t_1 values was obtained by using a 1K data block and time-proportional phase incrementation (TPPI) to ensure phase-sensitive line shapes with quadrature-phase detection in both frequency dimensions. Interferograms were zero-filled to 1K, and 3 Hz line-broadening was

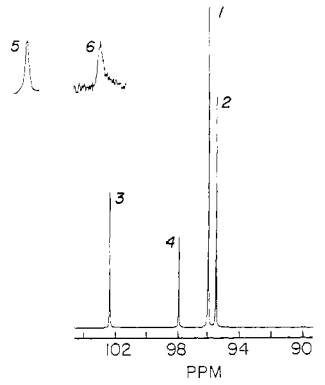

Figure 1. The ^{1}H-decoupled ^{13}C NMR spectrum (75 MHz) of D-[1-^{13}C]talose in aqueous solution, showing only signals due to the enriched C1 carbons. Six signals are observed and are assigned as shown to four cyclic (**1–4**) and two linear forms (**5**, **6**) (see Scheme I). The C1 signals of **5** and **6** (inset) are observed at 91.2 and 204.2 ppm, respectively (see text).

Scheme I

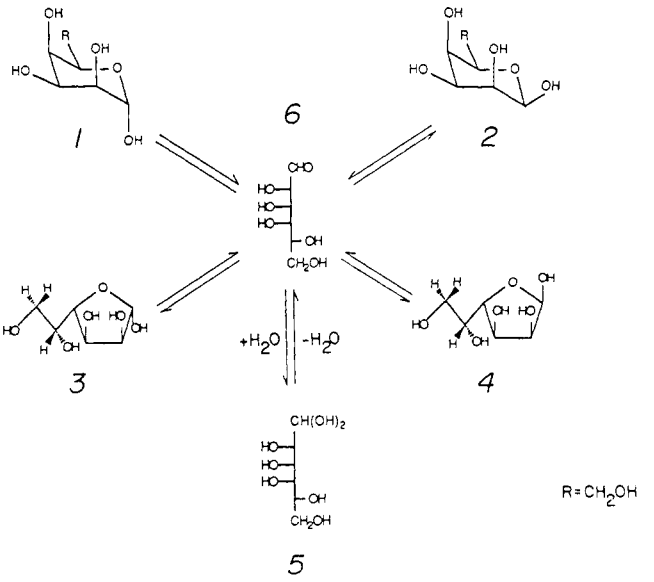

(14) Snyder, J. R.; Serianni, A. S. *Carbohydr. Res.* **1987**, *166*, 85.
(15) Huang, Y.; Macura, S.; Ernst, R. R. *J. Am. Chem. Soc.* **1981**, *103*, 5327.
(16) Anderson, L.; Garver, J. C. *Adv. Chem. Ser.* **1973**, *No. 117*, 20.
(17) Serianni, A. S.; Nunez, H. A.; Barker, R. *Carbohydr. Res.* **1979**, *72*, 71.
(18) Serianni, A. S.; Barker, R. Synthetic Approaches to Carbohydrates Enriched with Stable Isotopes of Carbon, Hydrogen and Oxygen. In *Isotopes in the Physical and Biomedical Sciences*; Buncel, E., Jones, J., Eds.; Elsevier: New York, 1987; p 211.
(19) Angyal, S. J.; Bethell, G. S.; Beveridge, R. J. *Carbohydr. Res.* **1979**, *73*, 9.
(20) Hodge, J. E.; Hofreiter, B. T. *Methods Carbohydr. Chem.* **1962**, *1*, 380.
(21) Stanek, J.; Cerný, M.; Kocourek, J.; Pacák, J. *The Monosaccharides*; Academic Press: New York, 1963.
(22) Serianni, A. S.; Barker, R. *Can. J. Chem.* **1979**, *57*, 3160.
(23) Ball, D. H. *J. Org. Chem.* **1966**, *31*, 220.
(24) Hayes, M. L.; Pennings, N. J.; Serianni, A. S.; Barker, R. *J. Am. Chem. Soc.* **1982**, *104*, 6764.
(25) Serianni, A. S.; Clark, E. L.; Barker, R. *Carbohydr. Res.* **1979**, *72*, 79.
(26) Morris, G. A.; Hall, L. D. *J. Am. Chem. Soc.* **1981**, *103*, 4703.
(27) (a) Johnston, E. R.; Dellwo, M. J.; Hendrix, J. *J. Magn. Reson.* **1986**, *66*, 399. (b) **R** represents a rate matrix that contains chemical exchange and longitudinal relaxation terms. The **R** matrix is calculated directly from an **A** matrix of normalized peak amplitudes by an eigenvalue–eigenvector method. The details of these calculations are given in ref 27a.

Table I. ^1H and ^{13}C NMR Chemical Shift Assignments[a] for D-Talose in ^2H_2O

compound	chemical shift, ppm						
	H1	H2	H3	H4	H5	H6	H6′
α-furanose	5.22	4.02	4.35	~3.92		3.72	3.63
β-furanose	5.35	4.13	4.21	4.08		3.68	3.61
α-pyranose	5.26	3.85	3.94	~3.92	4.08	3.81	3.77
β-pyranose	4.80	3.93	3.80	~3.85	3.62	3.83	3.78

compound	chemical shift, ppm					
	C1	C2	C3	C4	C5	C6
α-furanose	102.5	76.7	72.09	83.3	73.3	64.3
β-furanose	98.0	72.3	72.15	83.9	72.6	64.4
α-pyranose	96.2	72.2	66.6	71.1	72.6	63.0
β-pyranose	95.7	73.0	69.9	70.1	77.1	62.7

[a] ^1H values are relative to internal sodium 3-(trimethylsilyl)-1-propanesulfonate and are accurate to ±0.01 ppm. ^{13}C values are referenced (external) to the anomeric carbon of β-D-[1-^{13}C]glucopyranose (97.4 ppm) and are accurate to ±0.1 ppm. H5′ and H6′ are defined as the more shielded hydroxymethyl proton.

added in each time domain prior to double Fourier transformation. Broad-band proton decoupling was employed throughout the entire 2D exchange sequence. Mixing times (t_m) and temperatures (°C) were 3 s and 27 °C for D-erythrose and 1.5 s and 64 °C for D-talose. The recycle time (acquisition time plus relaxation delay) in both cases was 17 s. Peak volumes were obtained by integrating in $F2$ and summing over $F1$. These volumes were used to calculate the elements of $\mathbf{R}$[27b] as described previously by Johnston et al.[27a] Every fifth $F1$ value has been plotted in the 2D stack plots.

Computer modeling of talose tautomerization was performed on an IBM 370/3033 mainframe computer at the Notre Dame Computing Center. The Fortran program, CHO-40, was kindly provided by Dr. Philip W. Wertz of the University of Iowa and used to simulate the approach to equilibrium of the four cyclic talose tautomers interconverting via the central (aldehyde) form. The description and implementation of this program has been published previously.[6a,16]

Results

A. NMR Signal Assignments, Solution Composition, and Pyranose Ring Conformations of D-Talose. The ^{13}C NMR spectrum (75 MHz) of D-[1-^{13}C]talose in aqueous solution (0.6 M talose, 50 mM acetate buffer, pH 4.0, 15% v/v ^2H_2O) at 28 °C is shown in Figure 1. The four anomeric carbon signals were assigned previously by Pfeffer et al.[28] to α-talofuranose **3** (102.5 ppm), β-talofuranose **4** (98.0 ppm), α-talopyranose **1** (96.2 ppm), and β-talopyranose **2** (95.7 ppm) (Scheme I). These assignments were verified in this study by 2D ^{13}C–^1H shift correlation spectroscopy (data not shown) using reported ^1H chemical shift assignments.[29] In addition to the cyclic forms, the C1 signals of talose hydrate **5** and aldehyde **6** were observed at 91.2 and 204.2 ppm, respectively (Figure 1). These latter signals can be assigned with confidence, since the C1 carbons of the linear forms of aldoses resonate at characteristic regions of the ^{13}C spectrum.[3b,4,13]

Firm assignments of the nonanomeric proton and carbon resonances of the cyclic forms of talose have not been made previously, although several studies[28-31] addressed this problem. To make these assignments, the ^1H-decoupled ^{13}C NMR spectra of D-talose and D-[1-^{13}C]talose (unenriched region) were obtained (data not shown). A comparison of these spectra permitted an unequivocal identification of the C2 and C6 carbon signals; the assignment of these carbons (Table I) to specific cyclic forms was based on relative signal intensities and on previously described correlations between magnitudes of ^{13}C–^{13}C couplings and monosaccharide structure.[31] A 2D ^{13}C–^1H chemical shift correlation map was obtained to correlate proton multiplets at low resolution with specific carbon resonances, and resolution-enhanced 620-MHz ^1H NMR spectra of D-talose and D-[3-^{2}H]talose were obtained to assign these multiplets to specific protons. In contrast

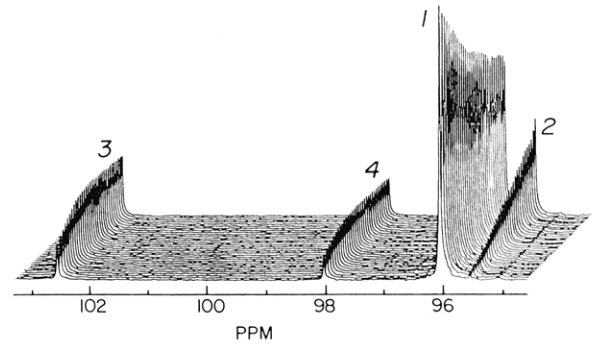

Figure 2. Typical time-lapse ^{13}C NMR experiment to obtain rates of equilibration of α-D-[1-^{13}C]talopyranose in aqueous solution with the remaining three cyclic forms. The loss of intensity of the α-pyranose (**1**) signal is accompanied by a rapid increase in intensity of the furanose (**3** and **4**) signals, followed by the appearance of the β-pyranose signal (**2**).

to the spectrum obtained on the natural compound, the ^1H spectrum of D-[3-^{2}H]talose at 620 MHz was amenable to nearly complete interpretation. Using the ^1H assignments (Table I) and the ^{13}C–^1H shift correlation map, the remaining carbon assignments (C3–C5) were made (Table I). These assignments confirm those reported recently[31] from an analysis of ^{13}C–^{13}C couplings in D-[1-^{13}C]talose.

The utility of ^{13}C–^{13}C coupling in studies of aldopyranose conformation is clearly illustrated in assessing the conformations of the talopyranoses. The $^3J_{HH}$ values for talopyranose anomers (Table II) are only sufficient to establish the conformation of α-talopyranose **1**. In **1**, H1 and H2 are diequatorial in the $^4C_1$ conformer and diaxial in the $^1C_4$ conformer. Therefore, $^3J_{H1,H2}$ is sufficient to distinguish these two forms, with the observed small coupling (1.9 Hz) consistent with a $^4C_1$ conformer. On the other hand, H1 and H2 for β-talopyranose **2** are axial–equatorial in both chair forms, making $^3J_{H1,H2}$ insufficient for a conformational assignment. More importantly, none of the remaining $^3J_{HH}$ values ($^3J_{H2,H3}$, $^3J_{H3,H4}$, $^3J_{H4,H5}$) can distinguish $^4C_1$ from $^1C_4$ since the disposition of these proton pairs is the same (ax–eq) in both conformers. The $^4C_1$ conformation can be assigned to **2**, however, on the basis that $^3J_{C1,C6}$ = 4.2 Hz in β-D-[1-^{13}C]talopyranose,[31] indicating that C1 and C6 are antiperiplanar. C1 and C6 are gauche in $^1C_4$, and a smaller $^3J_{C1,C6}$ (<1.5 Hz) would be expected in this case. In addition, the presence of an uncommon but structurally informative long-range coupling between H2 and H4 (1.2 Hz) (Table II) indicates that these atoms are near-coplanar and oriented in the W-shaped arrangement[32] found only in the $^4C_1$ conformer. Unlike D-idose,[13] the available coupling data for talopyranoses in ^2H_2O do not indicate a significant contribution from nonchair conformers.

B. Ring-Opening Rate Constants of Talose Tautomers. Ring-opening rate constants (k_{open}) of talose anomers (in 50 mM acetate buffer,[33] pH 4.0, 15% v/v ^2H_2O) were determined at various temperatures by saturation-transfer ^{13}C NMR spectroscopy.[3b,4,13] Transfer of saturation was measured from C1 of talose aldehyde **6** to the C1 signals of the cyclic forms **1**–**4**. Rate constants obtained for **3** and **4** (Table III) were used to calculate activation energies of 11.1 ± 0.5 and 12.1 ± 0.5 kcal/mol, respectively. Ring-opening of **1** and **2** was much slower than ring-opening of **3** and **4**; under the conditions used, k_{open} for **1** and **2** were obtainable by saturation transfer only at an elevated temperature (71 °C) (Table III). Below 71 °C, transfer of saturation was negligible and k_{open} could not be measured reliably.

Ring-opening activation energies were obtained for **3** and **4** to permit an estimation of k_{open} over a range of temperatures (25–85 °C), with the reasonable assumption that the Arrhenius plot for

(28) Pfeffer, P. E.; Valentine, K. M.; Parrish, F. W. *J. Am. Chem. Soc.* **1979**, *101*, 1265.
(29) Angyal, S. J.; Pickles, V. A. *Aust. J. Chem.* **1972**, *25*, 1695.
(30) Angyal, S. J. *Adv. Carbohydr. Chem. Biochem.* **1984**, *42*, 15.
(31) King-Morris, M. J.; Serianni, A. S. *J. Am. Chem. Soc.* **1987**, *109*, 3501.
(32) Barfield, M.; Dean, A. M.; Fallick, C. J.; Spear, R. J.; Sternhell, S.; Westerman, P. W. *J. Am. Chem. Soc.* **1975**, *97*, 1482.
(33) Acetate buffer was chosen for these studies because the pH of these solutions is independent of temperature ($\Delta pH/\Delta T = 0$). See: Dawson, R. M. C.; Elliott, D. C.; Elliott, W. H.; Jones, K. M. *Data for Biochemical Research*; Oxford University Press, New York, 1969; p 481.

Table II. ^1H–^1H Spin-Coupling Constants[a] for D-Talose in ^2H_2O

compound	coupled nuclei									
	1,2	2,3	3,4	4,5	5,6	5,6′	6,6′	2,4	1,3	1,5
α-furanose	1.7	4.8	6.9		4.4	7.5	−11.7	0.5	0.4	
β-furanose	4.1	5.7	5.1	3.2	4.7	7.8	−11.7	0.4		
α-pyranose	1.9	3.2	3.2	1.3	7.6	4.5	−11.7	1.4	0.3	0.6[b]
β-pyranose	1.2	3.2	3.3	1.2	7.8	4.4	−11.8	1.2		

[a] Values are reported in hertz and are accurate to ±0.1 Hz. [b] This long-range coupling is tentative.

Table III. Ring-Opening Rate Constants[a] for Talose Anomers Determined by ^{13}C Saturation-Transfer NMR

compound	41 °C	50 °C	59 °C	71 °C	E_{act}[c]
α-D-talofuranose	0.092	0.17	0.27	0.44	11.1 (±0.5)
β-D-talofuranose	0.086	0.14	0.26	0.45	12.1 (±0.5)
α-D-talopyranose	*b*	*b*	*b*	0.06	15.9[d]
β-D-talopyranose	*b*	*b*	*b*	0.05	16.3[d]

[a] In s^{-1}; ±10%. Solution conditions: 0.6 M D-[1-^{13}C]talose in 50 mM sodium acetate/acetic acid buffer, pH 4.0, 15% v/v ^2H_2O. [b] Rate constants at these temperatures were too small to be measured by saturation transfer. [c] In kcal/mol. [d] Values obtained from ref 8.

Table IV. Equilibrium Constants and Ring-Opening Rate Constants Used for Computer Modeling of Talose Mutarotation

compound	equilib const[a] (±50%)	rate const[b] (±20%)
α-talofuranose	620	0.046[c]
β-talofuranose	390	0.037[c]
α-talopyranose	1370	0.0022[c] (0.0043)[d]
β-talopyranose	970	0.0017[c] (0.0019)[d]

[a] [Cyclic tautomer]/[aldehyde]. These values were calculated from equilibrium percentages given in the text; there is considerable uncertainty (±50%) in their absolute magnitudes because of the large uncertainty in the proportion of aldehyde; insignificant figures are kept because the relative values of K_{eq} are less uncertain. [b] In s^{-1}; ±20%. Solution conditions: 50 mM sodium acetate buffer, pH 4.0, 15% v/v ^2H_2O, 28 °C. [c] Obtained from extrapolation of rate constants given in Table III. [d] Rate constants that gave a best fit of time-lapse ^{13}C NMR data (Figure 3).

the 15 °C region above and below the experimental temperature limits remained linear, as demonstrated for other aldofuranoses.[3b] Linear extrapolation to temperatures below 71 °C for **1** and **2** was made, albeit with more error, using activation energies reported by other investigators[8] (Table III). In this fashion, k_{open} for **1**–**4** were estimated at 28 °C (Table IV) and used in the following studies.

C. Time-Lapse ^{13}C NMR Studies of α-D-[1-^{13}C]Talopyranose. Rates of conversion at 28 °C of α-D-[1-^{13}C]talopyranose **1** into β-D-[1-^{13}C]talopyranose **2**, α-D-[1-^{13}C]talofuranose **3**, and β-D-[1-^{13}C]talofuranose **4** were determined by time-lapse ^{13}C NMR (Figure 2). α-D-[1-^{13}C]Talopyranose **1** (109 mg) was dissolved in 2 mL of 50 mM acetate buffer containing 15% v/v ^2H_2O at pH 4.0 in a 10-mm NMR tube, and ^{13}C spectra were recorded at suitable time intervals. The proportion of each tautomer in solution was measured as a function of time by spectral integration. As shown in Figure 3, **3** and **4** were produced rapidly from **1** and exceeded their final equilibrium proportions early in the reaction. This behavior is characteristic of monosaccharides that exhibit "complex mutarotation", as noted previously by Wertz et al.[6a] for D-galactose. The predictability of this unusual feature is a useful monitor of the goodness-of-fit of computer models of the reaction (see below). At equilibrium at 28 °C, the solution contained 18.5 ± 0.5% α-talofuranose **3**, 11.6 ± 0.3% β-talofuranose **4**, 41.0 ± 1.1% α-talopyranose **1**, 29.0 ± 0.8% β-talopyranose **2**, 0.03 ± 0.01% hydrate **5**, and 0.03 ± 0.01% aldehyde **6**.

Anderson and co-workers[6a,16] have reported previously a computer program, CHO-40, to calculate unidirectional rate constants of galactose anomerization by fitting complex mutarotation data based on a model in which the four cyclic forms of galactose interconvert via the linear carbonyl form. In the context of this study, this program was used to predict rates of equilibration of α-talopyranose **1** with **2**–**4** using k_{open} values obtained by ST-NMR and equilibrium constants obtained by spectral integration. Calculated curves were then compared to the experimental curves obtained by time-lapse ^{13}C NMR.

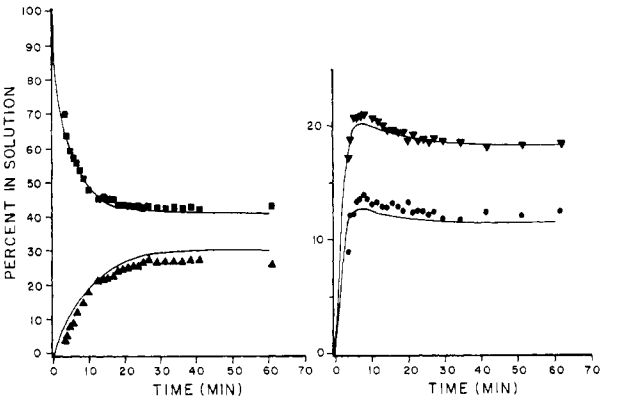

Figure 3. Comparison of time-lapse ^{13}C NMR data for the equilibration of α-D-[1-^{13}C]talopyranose in solution (Figure 2) (closed symbols) with computed equilibration curves generated from the CHO-40 computer program[6a,16] (smooth curves) (see text). A best fit of experiment with calculation was obtained by using rate constants given in Table IV (■, α-pyranose; ▲, β-pyranose; ▼, α-furanose; ●, β-furanose).

Equilibrium constants at 28 °C were calculated (Table IV) from the tautomeric percentages above, and furanose k_{open} values at 28 °C (Table IV) were determined from an Arrhenius plot of data in Table III. *Estimates* of pyranose k_{open} values at 28 °C (Table IV) were made using previously reported[8] activation energies of 15.9 and 16.3 kcal/mol for **1** and **2**, respectively. These constants were used to compute equilibration curves by the CHO-40 program. Some disparity between the predicted and observed equilibration curves was observed, which we attribute primarily to errors in the pyranose k_{open} values. This source of error was assessed by varying the ratio $k_{\alpha p,o}/k_{\beta p,o}$ over the range 0.25–2.5, keeping furanose k_{open}, K_{eq}, and $k_{\beta p,o}$ constant, to determine its effect on calculated equilibration curves. For ratios of 0.5 and 0.75, calculated curves for **1**–**4** deviated significantly from experiment; the disparity was greatest for **3** and **4**, which failed to overshoot their equilibrium concentrations in the calculated curves. As the ratio $k_{\alpha p,o}/k_{\beta p,o}$ approached 2.0, the furanoses began to overshoot their final equilibrium values, in closer agreement with experiment. Considering the overall behavior of **1**–**4**, a $k_{\alpha p,o}/k_{\beta p,o}$ ratio of 2.26 gave a reasonable fit of calculated and experimental data (Figure 3). Altering the ratio $k_{\alpha p,o}/k_{\beta p,o}$ by changing $k_{\beta p,o}$ instead of $k_{\alpha p,o}$ gave poorer fits of calculated and observed equilibration curves, even for ratios near 2.0.

Uncertainties in the quantitation of the linear aldehyde **6** will introduce errors in this treatment by affecting K_{eq} and thus k_{close} for each component reaction. The effect of linear aldehyde concentration on calculated equilibration curves was, therefore, examined with the CHO-40 program. Altering the percentage of **6** from 0.01% to 0.06% (experiment gives 0.03%) had virtually no effect on the predicted equilibration curves of **1**–**4**. This result is reasonable, since the rate-determining step in tautomer interconversion is ring-opening not ring-closing, and errors in k_{close} caused by K_{eq} errors will not effect equilibration behavior significantly. These facts lead us to conclude that the k_{open} values for **1** and **2** (Table IV) obtained from the fitting of calculated to observed equilibration curves are within ±20% of the true values.

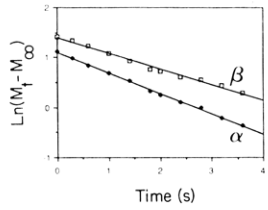

Figure 4. Semilogarithmic plot of ST-NMR data obtained for D-[1-^{13}C]erythrose, showing the effect of anomeric configuration on k_{open}. A detailed description of the use of this graphical treatment of ST-NMR data to obtain k_{open} is given in ref 3b and 4. Solution conditions: 0.25 M aldose, 50 mM sodium formate, pH 2.9, 15% v/v ^2H_2O, 27 °C. Ring-opening rate constants of 0.20 ± 0.01 and 0.081 ± 0.01 s^{-1} were calculated for α- and β-erythrofuranose, respectively.

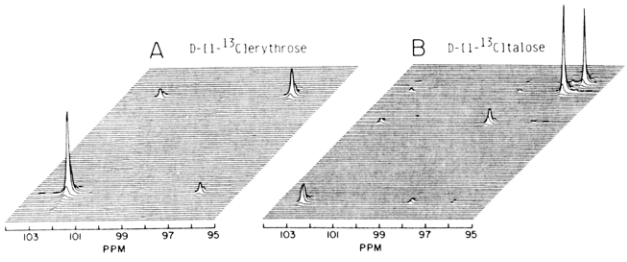

Figure 5. 2D ^{13}C chemical exchange maps for D-[1-^{13}C]erythrose (A) and D-[1-^{13}C]talose (B). The solution conditions for each experiment are given in the text. The 1D spectrum (C1 signals of cyclic forms) of each aldose is found along the diagonal. Cross peaks denote sites of chemical exchange and were used to extract overall rate constants of exchange between cyclic forms (Table V).

D. Overall Rates of Anomerization. Two-dimensional ^{13}C chemical exchange spectroscopy[15] has been used to measure the rate constants of interconversion (e.g., α-pyranose → β-furanose) between sugar tautomers,[34,35] although to date no studies of this kind have been reported on simple monosaccharides. Therefore, this method was first applied to the simple aldose, D-[1-^{13}C]-erythrose, which can form only two cyclic forms, α- and β-furanose, in solution.[3b] Equilibrium percentages of D-erythrose tautomers (0.25 M, 50 mM sodium formate, pH 2.9, 15% v/v ^2H_2O, 27 °C) were as follows: α-furanose, 25.5 ● 0.7%; β-furanose, 62.6 ± 1.7%; hydrate, 10.7 ± 0.3%; aldehyde, 1.2 ± 0.2%. The erythrose model system is limited to chemical exchange between two cyclic forms and allowed for a more straightforward comparison of kinetic data obtained from the 2D method and ST-NMR.

The ^{13}C saturation-transfer experiment on D-[1-^{13}C]erythrose (Figure 4) gave k_{open} values (determined from two separate experiments) of 0.20 ± 0.01 and 0.081 ± 0.01 s^{-1} for α- and β-furanose, respectively. From the equilibrium proportions above, k_{close} values of 4.3 ± 0.8 and 4.2 ± 0.8 s^{-1} were calculated for α- and β-furanose, respectively. These constants were used to calculate $k_{\alpha\beta}$ = 0.10 ± 0.04 s^{-1} and $k_{\beta\alpha}$ = 0.041 ± 0.02 s^{-1} from eq 1 derived assuming steady-state kinetics.

$$k_{\alpha\beta} = \frac{k_{\alpha o}k_{o\beta}}{k_{o\alpha} + k_{o\beta}} \qquad k_{\beta\alpha} = \frac{k_{\beta o}k_{o\alpha}}{k_{o\alpha} + k_{o\beta}} \tag{1}$$

These overall rate constants of erythrofuranose interconversion were compared to those measured directly by 2D ^{13}C chemical exchange spectroscopy[15,27a] (Figure 5A). This latter method gave $k_{\alpha\beta}$ = 0.11 ± 0.02 s^{-1} and $k_{\beta\alpha}$ = 0.045 ± 0.008 s^{-1}, in excellent agreement with $k_{\alpha\beta}$ and $k_{\beta\alpha}$ derived from the unidirectional rate constants obtained by ST-NMR.

A similar comparison was then made on D-[1-^{13}C]talose, which involves a more complex exchange network of four cyclic forms **1–4** interconverting via **6** (Figure 5B). Ring-opening rate constants for **3** and **4** at 64 °C (**3**, 0.33 ± 0.03 s^{-1}; **4**, 0.32 ± 0.03 s^{-1}) were calculated from an Arrhenius plot of data in Table III; k_{open} for **1** and **2** at 64 °C (**1**, 0.04 ± 0.02 s^{-1}; **2**, 0.03 ± 0.01 s^{-1}) were estimated in a similar fashion using activation energies[8] of 15.9 (α) and 16.3 (β) kcal/mol. Equilibrium proportions of talose tautomers at 64 °C were as follows: **1**, 34.3 ± 1.0%; **2**, 28.2 ● 0.8%; **3**, 22.8 ± 0.6%; **4**, 14.7 ± 0.4%; **6**, 0.10 ± 0.03%. From these proportions and k_{open}, k_{close} were calculated: **1**, 14 ± 10 s^{-1}; **2**, 8.5 ± 6.1 s^{-1}; **3**, 75 ± 45 s^{-1}; **4**, 47 ± 28 s^{-1}. Overall rate constants were calculated from k_{open} and k_{close}; for example, $k_{\alpha f,\beta f}$ was calculated from eq 2 derived assuming steady-state kinetics.

$$k_{\alpha f,\beta f} = \frac{k_{\alpha f,o}k_{o,\beta f}}{k_{o,\alpha f} + k_{o,\beta f} + k_{o,\alpha p} + k_{o,\beta p}} \tag{2}$$

Similar equations were used to calculate the 12 overall rate constants of interconversion between **1–4** (Table V). The 2D ^{13}C chemical exchange map of D-[1-^{13}C]talose at 64 °C was obtained (Figure 5B), from which overall rate constants of interconversion were measured directly (Table V). Good agreement was found between calculated (from ST-NMR data) and measured (2D exchange spectrum) rate constants.

Table V. Overall Rate Constants for the Interconversion of Talose Tautomers at 64 °C Determined by 2D ^{13}C Chemical Exchange Spectroscopy

reaction	$k \times 10^3$ (±20%),[a] s^{-1}	reaction	$k \times 10^3$ (±20%),[a] s^{-1}
αf → βf	110 (110)	βf → αf	190 (170)
αf → αp	45 (31)	αp → αf	24 (21)
αf → βp	16 (19)	βp → αf	11 (16)
βf → αp	51 (30)	αp → βf	15 (13)
βf → βp	24 (19)	βp → βf	9 (10)
αp → βp	*b* (2.3)	βp → αp	*b* (2.8)

[a] Solution conditions as in Table III. Values in parentheses were calculated from ring-opening and ring-closing rate constants at 64 °C (see text). [b] These rate constants were too small to be measured by 2D ^{13}C exchange spectroscopy.

Discussion

The primary objectives of this investigation were to measure and compare rate constants of aldose anomerization obtained from several NMR methods and, in doing so, gain further insight into the effects of pyranose and furanose structure and configuration on the kinetics of this important reaction. D-Talose was chosen for the investigation because all four cyclic hemiacetal forms (**1–4**) are present in aqueous solution as well as two less abundant but NMR-detectable linear forms (**5**, **6**) (Scheme I). Furthermore, talose can be synthesized with ^{13}C enrichment at C1 by established procedures,[17,18] and a pure anomer (α-pyranose **1**) can be obtained by crystallization from ethanol. These characteristics were essential to implement and compare the NMR methods used in this investigation.

A. Solution Composition and Conformation. Essential to this study were the detection and quantification of the hydrate **5** and aldehyde **6** forms of D-talose by ^{13}C NMR. The detection of these less abundant linear forms was feasible through the use of ^{13}C enrichment at the anomeric carbon and high-field ^{13}C NMR spectroscopy. This experimental approach has been applied previously to detect and quantify linear forms of erythrose,[3b] threose,[3b] pentose 5-phosphates,[4] fructose 6-phosphate,[4] 6-*O*-methylfructose 1-phosphate,[4] fructose 1,6-bisphosphate,[4] idose,[13] D-*glycero*-D-idoheptose,[13] D-fructose,[36] glucose,[37] 5-*O*-methylpentoses,[38] 5-deoxypentoses,[38] apiose,[14] ribose,[12,13,31] and altrose.[39] The detection and quantification of the linear forms of reducing sugars, although relatively unexplored, is important in defining the thermodynamics of aldose anomerization (e.g., $\Delta G°$, $\Delta H°$, and $\Delta S°$ of ring closure) and in measuring unidirectional rate

(34) Balaban, R. S.; Ferretti, J. A. *Proc. Natl. Acad. Sci. U.S.A.* **1983**, *80*, 1241.
(35) Fesik, S. W.; Kohlbrenner, W. E.; Gampe, R. T.; Olejniczak, E. T. *Carbohydr. Res.* **1986**, *153*, 136.
(36) Goux, W. *J. Am. Chem. Soc.* **1985**, *107*, 4320.
(37) Maple, S. R.; Allerhand, A. *J. Am. Chem. Soc.* **1987**, *109*, 3168.
(38) Snyder, J. R.; Serianni, A. S. *Carbohydr. Res.* **1987**, *163*, 169.
(39) Serianni, A. S., unpublished observation.

constants (k_{open}, k_{close}) by ST-NMR. The preferred conformations of the linear carbonyl forms of sugars in aqueous solution remain yet to be established, and this structural information will be valuable in interpreting anomerization kinetics, especially when the effects of alkyl substitution (e.g., "Thorpe–Ingold" effects[14,40]) are the focus of attention.

Although there are problems in assessing the conformation of **6**, it is possible to evaluate the conformations of the more abundant cyclic forms of talose, especially pyranoses **1** and **2**. Interpretation of the nonanomeric regions of the ^1H and ^{13}C spectra was possible through the use of 2D ^{13}C–^1H shift correlation spectroscopy, very high field ^1H NMR, and isotopically labeled molecules (D-[1-^{13}C]talose, D-[3-^2H]talose). The vicinal ^1H–^1H coupling data (Table II) are consistent with both talopyranoses (**1**, **2**) being conformationally stable. Both pyranoses assume the $^4C_1$ chair conformation, although long-range ^1H–^1H ($^4J_{HH}$) and ^{13}C–^{13}C ($^3J_{C1,C6}$) couplings were required to reach this conclusion for **2**. It is noteworthy that the conversion of D-talose to its C3 epimer, D-idose, causes a significant change in pyranose ring conformational behavior, with idopyranoses existing in both chair forms ($^4C_1$, $^1C_4$) to varying extents and in skew conformations (α-idopyranose).[13]

B. Comparison of Kinetic Constants Obtained by Different NMR Methods. Saturation-transfer NMR (ST-NMR) spectroscopy was first applied to carbohydrates by Serianni et al.[3b] as a means to obtain ring-opening rate constants in anomerizing systems. Two experimental tests have been applied previously to verify the accuracy of this method. First, Arrhenius plots generated from k_{open} values obtained by ST-NMR at lower temperatures (slow exchange) and by well-documented NMR line-broadening methods at higher temperatures (intermediate exchange) were found to be linear and yielded reasonable activation energies.[4] Second, the ^{13}C resonance line widths of the aldehyde forms of the tetroses calculated from k_{close} values were in good agreement with experimental line widths after field inhomogeneity contributions were taken into account.[3b,4] These observations provided evidence for the validity of the ST-NMR method, but further verification remained desirable.

Ring-opening rate constants are obtained directly by saturation-transfer, assuming that the method as applied to anomerization reactions is valid. Ring-closing rate constants are not measured directly, but are calculated from k_{open} and K_{eq} values for each component reaction. Consequently, k_{close} will be more prone to error than k_{open}, especially if the proportion of carbonyl form in solution is small and thus more difficult to quantify. For talose, however, the ST-derived rate constants appear accurate despite the low abundance of **6** in solution. This conclusion is based on two results. First, the overall rate constants calculated from ST-derived unidirectional rate constants agree with corresponding values determined independently under the same solution conditions by 2D ^{13}C chemical exchange spectroscopy (Table V). Second, rates of equilibration of α-D-talopyranose **1** with the remaining cyclic anomers **2**–**4** are predicted accurately from ST-derived rate constants. We conclude that, notwithstanding the errors inherent to each method, ST-NMR, 2D exchange spectroscopy, and computer-fitted time-lapse ^{13}C NMR give comparable results when implemented properly and should provide a powerful experimental triad to be exploited in future studies of carbohydrate anomerization.

There are inherent experimental limitations to each method used in this study, and consequently the exact duplication of experimental conditions that is preferred in comparative studies of this type could not be achieved. For example, for the time-lapse ^{13}C experiment, solution conditions (pH, temperature) had to be chosen to prevent significant equilibration during the time interval between dissolving α-D-[1-^{13}C]talopyranose **1** and initiating the data collection (~3 min). Unfortunately, these solution conditions were found to be unsatisfactory for saturation-transfer measurements (i.e., k_{open} values were too small to measure). This problem could not be avoided despite considerable effort to find mutually compatible conditions. Consequently, ST-NMR measurements had to be made at higher temperatures and Arrhenius plots used to extrapolate to the time-lapse solution conditions. A smaller temperature correction was also necessary to compare saturation-transfer and 2D ^{13}C chemical exchange experiments in order to allow the measurement of most exchange rates (with the exception of pyranose–pyranose interconversion) by the latter technique.

The typical reaction scheme (eq 3) used to describe carbohydrate anomerization involves two cyclic forms interconverting via a linear carbonyl form. A more complete description, however,

$$\text{cyclic}_1 \rightleftharpoons \text{linear} \rightleftharpoons \text{cyclic}_2 \qquad (3)$$

would include the conformational dynamics of the linear form, which involves bond rotation to expose alternate faces of the carbonyl carbon and/or reversible relaxation of a pseudoacyclic linear form, present immediately after ring-opening, to a more extended linear conformation. In general, these conformational processes are expected to be much faster than ring-opening and -closing, and thus not rate-limiting for anomerization. However, in some cases (e.g., where bulky substituents slow/limit the conformational interconversion of linear forms, or in enzyme-catalyzed anomerization), this process could compete with ring-opening and -closing and thus be kinetically significant. However, in these instances, as long as the acyclic form is a minor component of the system, the overall rate constants calculated from ST-derived unidirectional rate constants should be the same as those obtained directly by 2D chemical exchange spectroscopy. In addition, the 2D chemical exchange experiment treats anomerization as a two-site exchange problem involving pairs of cyclic forms, that is, the linear form, although an obligatory intermediate in the interconversion, is not treated explicitly in the experiment. This situation is probably valid as long as magnetization transfer between the cyclic forms is not affected by the presence of the linear form, a condition satisfied when the proportion of the linear form in solution is small. However, at higher concentrations of linear form, the reaction must be treated as a three-site exchange problem.

C. Talose Anomerization. Like idose and altrose,[13,29,30] aqueous solutions of D-talose contain four cyclic forms in comparable proportions, and these aldohexoses provide convenient systems to study simultaneously the kinetics of furanose and pyranose anomerization. We have been interested in the effects of ring structure and configuration on reaction rates, as these effects may point to important mechanistic features of ring-opening and ring-forming reactions in general.

Time-lapse equilibration studies of α-D-[1-^{13}C]talopyranose **1** showed a rapid production of talofuranoses **3** and **4**, followed later by the β-pyranose **2** (Figures 2 and 3). This result suggests that rates of pyranose–furanose interconversion are greater than those of pyranose–pyranose interconversion. Furthermore, the rapid and concomitant generation of both furanose anomers in proportions similar to those found at chemical equilibrium implies that the rate of furanose–furanose interconversion is comparable to, or greater than, pyranose–furanose interconversion. Under the conditions used in this study, the increase in concentration of both furanose anomers was not strictly hyperbolic. Instead, their concentrations reached maximal values early during the equilibration and eventually decayed to their equilibrium values as **2** began to accumulate. This behavior is a direct consequence of a slow pyranose–pyranose interconversion rate. Early in the equilibration, **3** and **4** compete only with **1**, producing a transient three-site system (plus open chain) in nonthermodynamic steady state. A similar overshoot in furanose concentration was observed previously in galactose anomerization by Wertz et al.,[6a] who predicted this behavior to depend on the ratio of the pyranose ring-opening rate constants, $k_{\alpha p,o}/k_{\beta p,o}$. From computer modeling, these investigators showed that overshooting occurred as this ratio approached 2.0.

(40) (a) Beesley, R. M.; Ingold, C. K.; Thorpe, J. F. *J. Chem. Soc.* **1915**, *107*, 1080. (b) Allinger, N. L.; Zalkow, V. *J. Org. Chem.* **1960**, *25*, 701. (c) Jager, J.; Graafland, T.; Schenk, H.; Kirby, A. J.; Engberts, J. B. F. N. *J. Am. Chem. Soc.* **1984**, *106*, 139.

The above qualitative conclusions have been validated and quantified in this study through the use of ST-NMR and 2D ^{13}C chemical exchange spectroscopy. For talose, rate constants of furanose–furanose interconversion are 2–20 times greater than those for pyranose–furanose interconversion, while pyranose–pyranose interconversion is 5–20 times slower than pyranose–furanose interconversion (Table V). Furthermore, the best fit of time-lapse ^{13}C NMR data to calculated equilibration curves (Table IV, Figure 3), especially with respect to furanose overshooting, is obtained when $k_{\alpha p,o}/k_{\beta p,o}$ = 2.26, a value consistent with previous predictions.[6a]

An inspection of the unidirectional rate constants for talose anomerization shows that k_{open} for pyranoses is considerably slower than for furanoses, which accounts for the lower overall pyranose–pyranose interconversion rates. Furthermore, there appears to be a dependence of anomeric configuration on these rates, with $k_{\alpha f,o}/k_{\beta f,o}$ = 1.2 and $k_{\alpha p,o}/k_{\beta p,o}$ = 2.3. The effect of talofuranose anomeric configuration on k_{open} differs from our previous observations on tetro- and pentofuranoses in which anomers having O1,O2 cis were more predisposed toward ring-opening than corresponding anomers having these groups trans,[3b,38] as observed in the configurationally related 5-*O*-methyl-α-D-ribofuranose **7** and 5-*O*-methyl-β-D-ribofuranose **8**. The opposite relationship is found for talofuranoses, where **3** (related configurationally to **8**) ring-opens faster than **4** (related configurationally to **7**), although the difference is small. It is possible that exocyclic structure at C4 and ring conformation may affect relative ring-opening rates between furanose anomers, although k_{open} values for idofuranoses and 5-*O*-methyl-D-xylofuranoses showed a similar dependence on anomeric configuration.[13] On the other hand, a consistency between **3**, **4** and **7**, **8** is observed with respect to k_{close}, with O1,O2 trans anomers (**3**, **8**) reacting 1.5–2.0 times faster than O1,O2 cis anomers (**4**, **7**).

In a previous study of D-idose,[13] we showed that furanose cyclization occurs more rapidly than pyranose cyclization. This observation differed from earlier conclusions made by Wertz et al.[6a] based on computer-modeling studies of galactose anomerization where k_{close} of furanoses and pyranoses were found to be comparable. The present study provides further experimental evidence that furanose ring formation is more favored kinetically than pyranose ring formation, at least in the aldohexoses.

Considerably less is known at present about the effect of pyranose anomeric configuration on k_{open} and k_{close}. For talose, **1** undergoes ring-opening and -closing more readily than **2** even though **1** is more thermodynamically stable than **2**. The same is true for talofuranoses, that is, **3** is favored over **4** both kinetically and thermodynamically. Further studies are needed, however, to more firmly identify the structural factors affecting pyranose anomerization kinetics.

Conclusions

This study has shown that saturation-transfer NMR, computer-fitted time-lapse ^{13}C NMR, and 2D ^{13}C chemical exchange spectroscopy yield an internally consistent kinetic picture of aldohexose anomerization, and it provides a firm foundation on which to apply these experimental approaches to anomerization studies in general. Previous qualitative treatments of the effect of aldose structure on tautomer interconversion rates and dissolution behavior have been validated and quantified with new data provided by these methods.

We have also shown that complex ^{1}H and ^{13}C NMR spectra of aldohexoses can be interpreted almost completely with the use of 2D ^{13}C–^{1}H shift correlation spectroscopy and very high field ^{1}H NMR. These methods are enhanced when isotopically labeled (^{13}C, ^{2}H) molecules are employed. This approach should prove practical in future studies of other "complex" aldohexoses (e.g., altrose). With assistance from ^{13}C-enriched molecules, ^{13}C NMR is well-suited for the detection and quantification of the linear hydrate and carbonyl forms of sugars in solution which are essential to the measurement of thermodynamic and kinetic parameters of the anomerization reaction.

Acknowledgment. We thank Dr. Mishra of the NMR Facility for Biomedical Studies, Department of Chemistry, Carnegie Mellon University, for his assistance in obtaining the 620-MHz ^{1}H NMR spectra and Dr. Philip W. Wertz, University of Iowa, for providing a copy of the CHO-40 computer program. We thank Mr. Donald Schifferl for making the required hardware modifications on our NT-300 to conduct ^{13}C ST-NMR experiments, the Notre Dame Computing Center for use of the IBM 370/3033 mainframe computer, and Rosemary Patti for typing the manuscript. This work was supported by the Research Corp. (Grant 10028) and the National Institutes of Health (Grant GM 33791).

Registry No. D-Talose, 2595-98-4.

Supplementary Material Available: A 2D ^{13}C–^{1}H chemical shift correlation map of D-talose (Figure S1), high-resolution cross-correlation ^{1}H NMR spectra (620 MHz) of D-talose and D-[3-^{2}H]talose (Figure S2), and expanded and assigned regions of the 620-MHz ^{1}H NMR spectrum of D-[3-^{2}H]talose (Figure S3) (4 pages). Ordering information is given on any current masthead page.